Spontaneous opticospinal encephalomyelitis in a double-transgenic mouse model of autoimmune T cell/B cell cooperation

Gurumoorthy Krishnamoorthy,[1] Hans Lassmann,[2] Hartmut Wekerle,[1] and Andreas Holz[1]

[1]Department of Neuroimmunology, Max Planck Institute for Neurobiology, Martinsried, Germany. [2]Division of Neuroimmunology, Center for Brain Research, Medical University of Vienna, Vienna, Austria.

We describe a double-transgenic mouse strain (opticospinal EAE [OSE] mouse) that spontaneously develops an EAE-like neurological syndrome closely resembling a human variant of multiple sclerosis, Devic disease (also called neuromyelitis optica). Like in Devic disease, the inflammatory, demyelinating lesions were located in the optic nerve and spinal cord, sparing brain and cerebellum, and the murine lesions showed histological similarity with their human correlates. OSE mice have recombination-competent immune cells expressing a TCR-αβ specific for myelin oligodendrocyte glycoprotein (MOG) aa 35–55 peptide in the context of I-A^b along with an Ig J region replaced by the recombined heavy chain of a monoclonal antibody binding to a conformational epitope on MOG. OSE mouse B cells bound even high dilutions of recombinant MOG, but not MOG peptide, and processed and presented it to autologous T cells. In addition, in OSE mice, but not in single-transgenic parental mice, anti-MOG antibodies were switched from IgM to IgG1.

Introduction

MS is the most important demyelinating disease in the northern hemisphere. It arises without known trigger and either progresses in isolated bouts or worsens steadily from the very beginning. In the classical form of MS the demyelinating plaques are spread throughout the CNS. Usually the plaques appear in certain preferred locations, such as around the periventricular areas, but there are also variants in which the disease is limited to individual regions of the CNS. In Devic disease, for example, the lesions are restricted to the optic nerve and the spinal cord, sparing the cerebrum and the cerebellum (1). MS and its subgroups also have distinct histological patterns of pathological changes (2).

The factors determining onset, course, distribution, and cellular composition of autoimmune lesions in MS are largely unknown. In particular, it is unclear which processes are involved in triggering the onset of the disease and which drive inflammation during the further course of the disorder. While some investigators link the trigger(s) of MS to microbial infection (3), the opposite has been proposed as well, namely that the propensity to autoimmune disorders is related to the decreasing prevalence of infections (4). Our ignorance of these vital issues is largely due to the lack of suitable experimental models that would develop human CNS disease spontaneously and reproduce its essential clinical and structural aspects.

Here we describe a double-transgenic mouse strain that may fill this gap. These animals spontaneously developed a neurological condition that strikingly resembled the Devic variant of human MS. The majority of these opticospinal EAE (OSE) mice had a paralytic disease caused by inflammatory demyelinating lesions in the spinal cord and the optic nerve. The causative CNS lesions, again much like human Devic lesions, sometimes contained a high proportion of eosinophilic leukocytes besides T cells and macrophages.

Results

Spontaneous EAE-like disease in OSE double-transgenic mice. Myelin oligodendrocyte glycoprotein–specific (MOG-specific) TCR transgenic mice on a C57BL/6 background (TCR^{MOG} mice; also referred to as 2D2 mice; ref. 5) express a transgenic TCR recognizing MOG aa 35–55 peptide in the context of I-A^b on most $CD4^+$ T cells. TCR^{MOG} transgenic animals rarely have classic EAE, although a major proportion of the older ones develop optic neuritis. MOG-specific Ig heavy-chain knock-in mice on a C57BL/6 background (IgH^{MOG} mice; also referred to as Th mice) contain B lymphocytes that produce antibodies with the heavy chain of a demyelinating MOG-specific antibody (8.18C5) (6, 7). Despite high titers of pathogenic serum antibodies, the spontaneous development of autoimmunity has not previously been observed (8).

TCR^{MOG} and IgH^{MOG} single-transgenic animals were crossed, both on a C57BL/6 background. EAE-like signs (a disease score of at least 3; see Methods) were observed in 51% of the mice kept under specific pathogen–free (SPF) conditions (Figure 1) and in 46% of mice housed under conventional conditions (Supplemental Figure 1; supplemental material available online with this article; doi:10.1172/JCI28330DS1). All single-transgenic littermates remained healthy throughout the 12-week observation period (Figure 1). The mean maximum disease score among TCR^{MOG}×IgH^{MOG} double-transgenic animals, termed OSE (opticospinal EAE) mice, was 3.4 ± 1.2 with a mean onset at 6.1 ± 2.0 postnatal weeks. Female and male OSE mice developed EAE-like disease at similar rates (Figure 1). Neurological disease followed a chronic course with no marked remissions, and disease onset in the mice coincided with substantial weight loss (see Supplemental Figure 2).

There was no spontaneous EAE in F1 crosses of IgH^{MOG} mice with OVA-specific TCR transgenic mice on a C57BL/6 background

Nonstandard abbreviations used: FACS, fluorescence-activated cell sorting; IgH^{MOG} mice, MOG-specific Ig heavy-chain knock-in mice on a C57BL/6 background; MBP, myelin basic protein; MOG, myelin oligodendrocyte glycoprotein; OSE, opticospinal EAE; rMOG, recombinant MOG aa 1–125; SPF, specific pathogen–free; TCR^{MOG} mice, MOG-specific TCR transgenic mice on a C57BL/6 background; TCR^{OVA} mice, OVA-specific TCR transgenic mice on a C57BL/6 background.

Conflict of interest: The authors have declared that no conflict of interest exists.

Citation for this article: *J. Clin. Invest.* **116**:2385–2392 (2006). doi:10.1172/JCI28330.

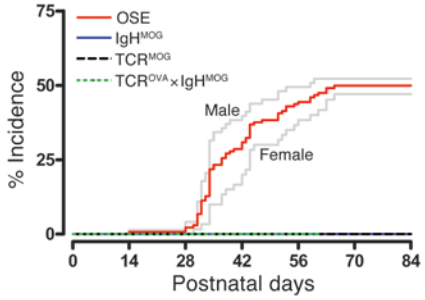

Figure 1
Spontaneous EAE-like disease in TCR^{MOG}×IgH^{MOG} double-transgenic (OSE) mice. Spontaneous incidence after birth of severe EAE-like disease (clinical score ≥3) was observed in double-transgenic mice housed under SPF conditions (red line; n = 133, 60 females and 73 males). Single-transgenic littermates (IgH^{MOG}, n = 69; TCR^{MOG}, n = 34) and TCR^{OVA}×IgH^{MOG} double-transgenic mice (n = 11) remained free of clinical signs during the observation period. Gray lines show disease incidence for male and female OSE mice. The difference in the disease kinetics between sexes was not statistically significant (P = 0.2263).

(TCR^{OVA} mice, also referred to as OT-II mice) specific for OVA aa 323–339 (9) (Figure 1) nor in OSE mice lacking MOG antigen ($MOG^{-/-}$ mice; ref. 10; data not shown).

The pathological CNS lesion. In OSE mice with spontaneous EAE kept under conventional conditions, CNS lesions were located almost exclusively in the optic nerve and in the spinal cord (Figure 2). The lesions were circumscribed rather than diffuse and were characterized by massive infiltration of inflammatory cells along with profound demyelination and moderate axonal loss. In sharp contrast, inflammation in the spinal cords and optic nerves in TCR^{MOG} and IgH^{MOG} single-transgenic littermates of the same age was sparse or absent. Only in exceptional animals was it associated with some perivascular tissue damage. Healthy OSE mice showed only sparse inflammatory infiltrates in the CNS (Supplemental Figure 3).

The inflammatory infiltrates were dominated by mononuclear cells (Figure 2). Immunocytochemistry identified macrophages and $CD4^+$ T cells, but only very few $B220^+$ B cells or $CD8^+$ T cells (Figure 2, L–O), in the optic nerve and the spinal cord. It is noteworthy that using the same antibody staining of the brain did not reveal immunoreactivity. In addition, some actively demyelinating lesions contained abundant eosinophilic granulocytes.

Double-transgenic mice that were kept under SPF conditions also showed profound inflammatory demyelination in their optic nerves and spinal cords. In addition, SPF-bred animals exhibited extensive inflammation that formed thick mononuclear infiltrates in the meninges and perivascular spaces. Demyelination was associated with mononuclear cell infiltration of the tissue, but eosinophilic granulocytes were generally absent (Supplemental Figure 4).

Activation of CNS-infiltrating $CD4^+$ T cells. In contrast to healthy TCR^{MOG} and IgH^{MOG} single-transgenic animals, which yielded only very few inflammatory cells, large numbers of inflammatory cells were recovered from the spinal cords of sick OSE mice. Percoll gradient–separated infiltrate cells were predominantly $CD4^+CD3^+$ T lymphocytes, along with a $CD11b^+$ macrophage/monocyte component (Figure 3). The $CD4^+$ T cells were stained by antibodies directed against Vα3.2 and Vβ11 (Figure 3F), the V region specificities of the transgenic TCR^{MOG} mouse.

Of note, $CD4^+CD3^+$ T lymphocytes from the CNS of sick OSE mice showed a highly activated phenotype indicated by the markers CD69 and CD25 (Figure 3D) as well as CD44 (data not shown). In contrast, CD3 and CD62L (data not shown) were partly downregulated. Splenic T cells from the same sick OSE animals were not activated (Figure 3B).

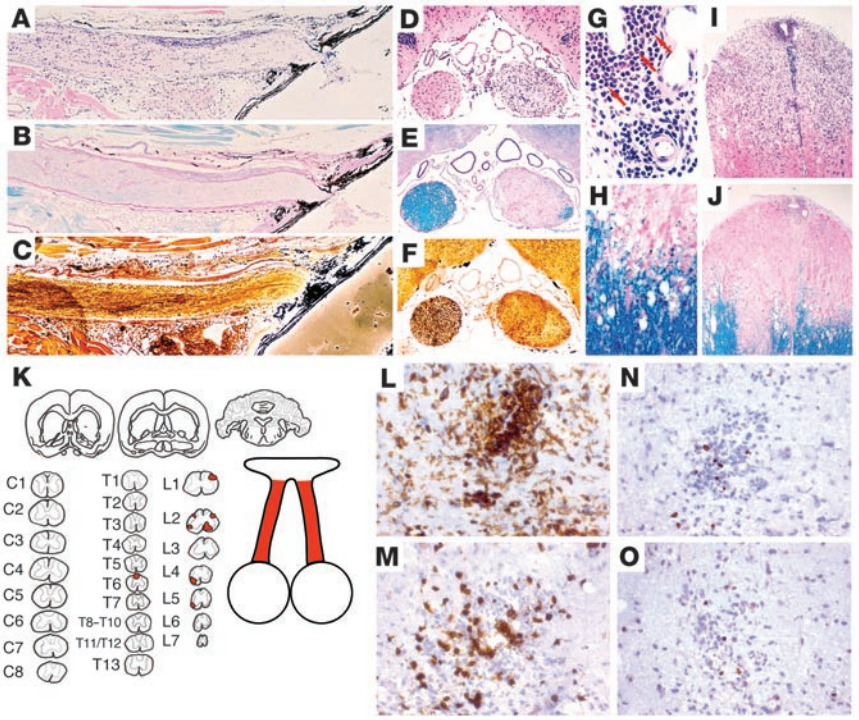

Figure 2
Histological analysis of the CNS from sick OSE mice. (**A**–**J** and **L**–**O**) The optic nerves (**A**–**F**) and spinal cords (**G**–**J** and **L**–**O**) from OSE mice that developed neurological disease in a non-SPF environment showed severe infiltration, demyelination, and axonal damage as visualized by H&E (**A**, **D**, **G**, and **I**), luxol fast blue (**B**, **E**, **H**, and **J**), and Bielschowsky silver impregnation (**C** and **F**). Arrows in **G** indicate eosinophilic granulocytes. (**K**) Demyelinating lesions (red shading) were specifically localized in the optic nerves and spinal cords of OSE mice, thus resembling the lesion distribution observed in human Devic disease. Cervical sections are labeled C1–C8; thoracic sections are labeled T1–T13; lumbar sections of the spinal cord are labeled L1–L7. (**L**–**O**) Cellular infiltrates were predominantly composed of $CD11b^+$ macrophages/microglia (**L**) and $CD4^+$ T cells (**M**), while only few $CD8^+$ T (**N**) and B cells (**O**) were found exclusively in the optic nerves and spinal cords of sick mice. Note that healthy OSE littermates remained free of demyelinating CNS lesions (see Supplemental Figure 3). Furthermore, OSE mice housed under SPF conditions showed slightly stronger infiltration/demyelination (see Supplemental Figure 4).

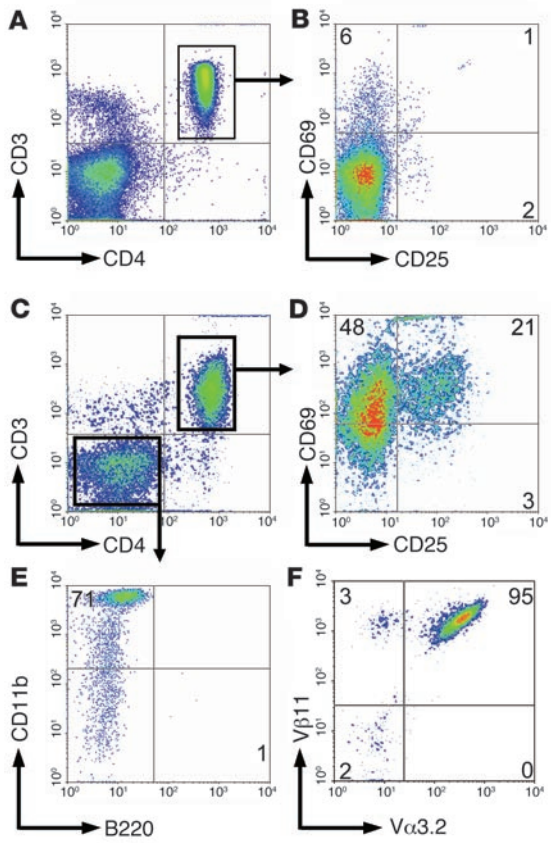

Figure 3
Activated pathogenic CD4+ T cells infiltrate the spinal cord of OSE mice. (**A**–**D**) Living splenocytes (**A** and **B**) and CNS mononuclear cells (**C** and **D**) isolated by Percoll gradient centrifugation from a sick OSE mouse were stained with CD4 and CD3 (**A** and **C**), and CD25 and CD69 expression was analyzed among gated CD4+CD3+ double-positive T cells (**B** and **D**). (**E**) Gated CD4–CD3– CNS cells were stained with anti-CD11b and anti-B220 in a separate reaction. (**F**) CD4+CD3+ T cells infiltrating the CNS of sick OSE mice predominantly expressed the pathogenic TCR composed of Vα3.2 and Vβ11 chains. Numbers indicate the percentage of stained cells in the respective quadrant. Flow cytometric data are representative of 7 sick OSE animals analyzed in 4 independent experiments.

Cytokine and chemokine expression in CNS lesions. Quantitative real-time PCR was used to compare the transcription of cytokines and chemokines in the spinal cords of OSE animals with spontaneous EAE and WT C57BL/6 mice with actively induced EAE. Both profiles were almost identical. The cytokine genes *IFN-γ* and *TNF-α* were substantially enhanced, while *IL-4*, *IL-5*, *IL-10*, *IL-13*, and *IL-17* transcripts remained practically undetectable (Figure 4). In healthy single-transgenic TCR^{MOG} and IgH^{MOG} littermates, none of these transcriptsæ were found.

The chemokines IP-10 and eotaxin were transcribed at similar high levels in sick OSE animals and C57BL/6 mice with MOG aa 35–55–induced EAE (Figure 4).

Enhanced anti-MOG response and cytokine production by lymphocytes from OSE mice. Spleen cells from OSE mice responded to recombinant MOG aa 1–125 (rMOG) much more efficiently than did TCR^{MOG} single-transgenic control cells (Figure 5A). Antigen doses of 0.02 μg/ml caused massive proliferation of double-transgenic splenocytes, while TCR^{MOG} single-transgenic cells required more than 100-fold protein concentrations. IgH^{MOG} single-transgenic splenocytes scarcely or only weakly responded to rMOG, even at high concentrations (Figure 5A).

In sharp contrast, the immunodominant peptide MOG aa 35–55 was recognized equally by OSE and single-transgenic TCR^{MOG} mice (Figure 5B). Both required relatively high peptide concentrations for measurable activation, whereas spleen cells from single-transgenic IgH^{MOG} mice completely failed to respond to MOG aa 35–55.

In an initial attempt to elucidate the relative contribution of MOG-reactive T and B cells to the enhanced reactivity of OSE spleen cells, single-transgenic IgH^{MOG} splenocytes were mixed with cells from single-transgenic TCR^{MOG} spleens. The combination of both single-transgenic populations potentiated rMOG reactivity (see Supplemental Figure 5A). A similar supra-additive effect was produced by combining B and T cells purified (>90% by fluorescence-activated cell sorting [FACS] analysis) from single-transgenic TCR^{MOG} and IgH^{MOG} spleens. Figure 5C shows that the combination of MOG-reactive T and B cells from single-transgenic TCR^{MOG} and IgH^{MOG} mice fully reproduced the high reactivity of unseparated double-transgenic OSE mouse splenocytes. In contrast, transgenic T cells from TCR^{MOG} mice combined with nontransgenic B cells and transgenic B cells from IgH^{MOG} mice together with nontransgenic T cells showed comparable proliferative responses (Figure 5C). Finally, the mixing of highly purified transgenic T and B cells from OSE mice restored the enhanced proliferation kinetics of unseparated OSE splenocytes (Supplemental Figure 5B).

The contribution of transgenic T or B lymphocytes to the proliferative response of rMOG was determined by labeling OSE splenocytes with CFSE and exposing them to optimal antigen doses in vitro. Both T and B cells were driven to proliferate (Figure 5D). In

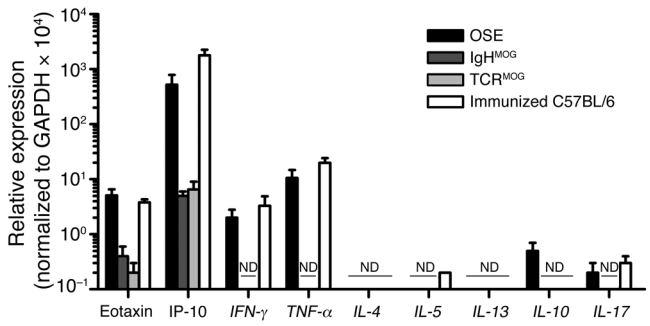

Figure 4
Cytokine milieu in the spinal cords of sick OSE mice. Relative expression level of various cytokine and chemokine genes was assessed by quantitative PCR in the spinal cords of sick OSE mice ($n = 5$; clinical score ≥3), healthy IgH^{MOG} mice ($n = 3$), healthy TCR^{MOG} mice ($n = 3$), and C57BL/6 mice immunized with MOG aa 35–55 ($n = 3$; clinical score ≥3). Error bars represent SEM from the measurement of individual animals within each experimental group. ND, no gene expression was detectable.

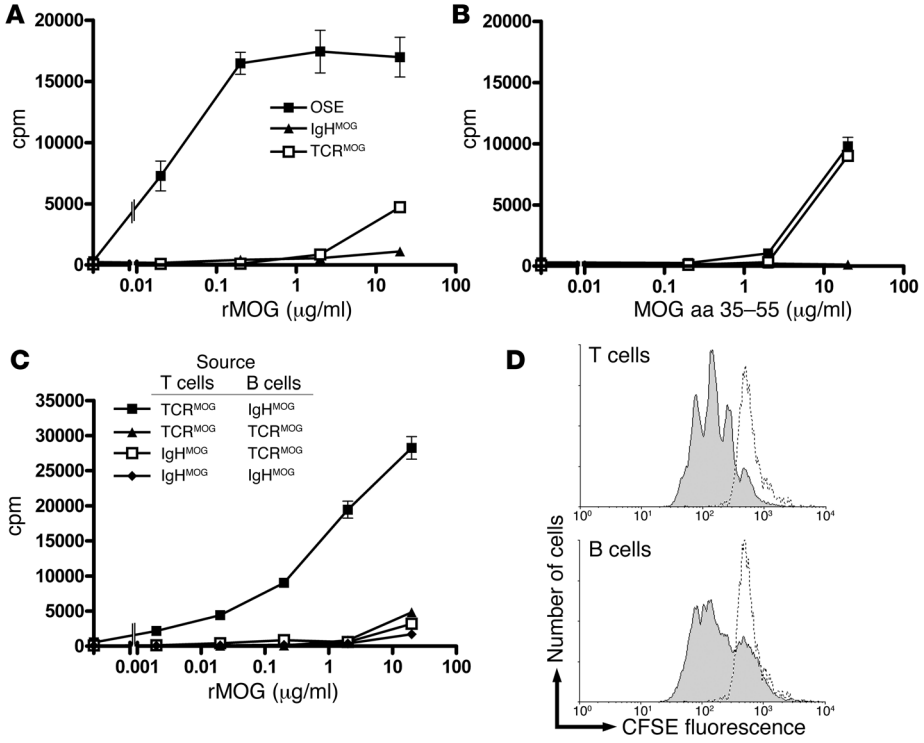

Figure 5

Enhanced autoreactivity of lymphocytes from OSE mice to rMOG. (**A** and **B**) Proliferation of splenocytes from OSE, TCR^{MOG} single-transgenic, and IgH^{MOG} single-transgenic mice in response to increasing concentrations of (**A**) rMOG and (**B**) MOG aa 35–55 peptide. (**C**) Proliferation of $CD4^+$ T cells and B cells isolated from IgH^{MOG} and TCR^{MOG} single-transgenic mice that were combined as indicated after their purification (>90% purity) and stimulated with increasing amounts of rMOG. Note that the combination of MOG-reactive T and B cells caused a substantial increase in proliferation in response to rMOG, comparable to that of OSE splenocytes. (**D**) Splenocytes from an OSE mouse were labeled with CFSE and stimulated with optimal concentrations of rMOG in vitro. The dilution of cellular CFSE due to proliferation of live-gated $CD4^+CD3^+$ T lymphocytes (top) and live-gated $CD19^+$ B lymphocytes (bottom) is shown. Splenocytes that remained without stimulus are represented by dotted lines. In **A**–**C**, each data point was run in triplicate, and error bars indicate SEM. Experiments in **A** and **B** were replicated on multiple occasions (>10), those in **C** and **D** were repeated twice.

addition, both responding lymphocyte populations were activated. T cells expressed CD25, and B cells CD86, as activation markers (Supplemental Figure 6).

The cytokines secreted by MOG-stimulated splenocytes from OSE mice in vitro were measured by ELISA. Predominantly, the cytokines IL-2, IFN-γ, and IL-17 (albeit to a lesser extent) were released from OSE and TCR^{MOG} T cells in the dose-response pattern previously found in proliferation assays. In contrast, IL-4 was only marginally detectable in the supernatants, while low levels of IL-5 were seen in responding OSE but not TCR^{MOG} T cell cultures (Figure 6A). While stimulation with high doses of MOG aa 35–55 peptide released IL-2, IFN-γ, IL-17, and IL-5 cytokines from OSE splenocytes, low peptide doses did not trigger any detectable cytokine secretion (Figure 6B).

Production of anti-MOG autoantibodies. OSE mice, either with or without EAE, did not visibly differ in absolute number and cellular composition of splenocytes (Supplemental Table 1) or in cellular function (data not shown). In particular, the capability of MOG-specific transgenic B cells to bind rMOG was unaltered during disease onset and progression. Finally, the proliferation kinetics and expression of T and B cell activation markers as well as the quantity and quality of cytokines secreted by transgenic splenocytes in response to rMOG remained unaffected by the clinical status of OSE animals (our unpublished observations).

However, OSE mice differed strikingly from age-matched single-transgenic IgH^{MOG} or double-transgenic TCR^{OVA}×IgH^{MOG} mice by their high titers of the IgG1 isotype of anti-MOG autoantibody (Figure 7). While TCR^{MOG} single-transgenic mice did not spontaneously develop any anti-MOG antibodies (Supplemental Figure 7), most of the anti-MOG autoantibodies in single-transgenic IgH^{MOG} and in TCR^{OVA}×IgH^{MOG} mice were IgM.

The onset of clinical EAE did not affect the level or nature of anti-MOG IgG1 antibodies (Figure 7). Furthermore, longitudinal studies of individual OSE mice showed constant amounts of MOG-specific IgM, IgG1, and IgG2 antibodies (see Supplemental Figure 7). Finally, OSE mice that lacked MOG antigen (i.e., triple-transgenic TCR^{MOG}×IgH^{MOG}×$MOG^{-/-}$ animals) exhibited increased amounts of anti-MOG IgG1 serum antibodies, indicating that their generation occurred independently of MOG antigen (Figure 7).

Discussion

The OSE double-transgenic mouse EAE model described here stands out in several respects. The inflammatory demyelinating disease developed spontaneously, it resulted from pathogenic interaction between myelin autoimmune T and B cells, and the distribution and cellular composition of its lesions resembled that of Devic disease, a variant of human MS.

Spontaneously developing organ-specific autoimmune disease models in rodents are rare. Most notably, the NOD mouse develops type 1 diabetes mellitus at variable frequency within 40 weeks (4). Spontaneous autoimmune disease was also reported in the CNS. Spontaneous EAE was seen in transgenic mice with a TCR specific for myelin basic protein (MBP) in the context of $I\text{-}A^u$ (11, 12) at low frequency: <15% under conventional and 0% under SPF conditions (11). Higher frequencies were observed in the absence of regulatory lymphocytes in double-transgenic MBP-specific TCR transgenic mice on a B10.PL background (TCR^{MBP}) crossed with recombinase activating gene–deficient mice (TCR^{MBP}×$RAG^{-/-}$ mice; ref. 12). Of interest, these transgenic mice, very similar to our double-transgenic model, showed activated antigen-specific T cells only in the CNS that remained undetectable in peripheral organs (12).

OSE mice developed the disease at rates of about 50% within the first 10 weeks of age, although neither of the 2 parental T and B

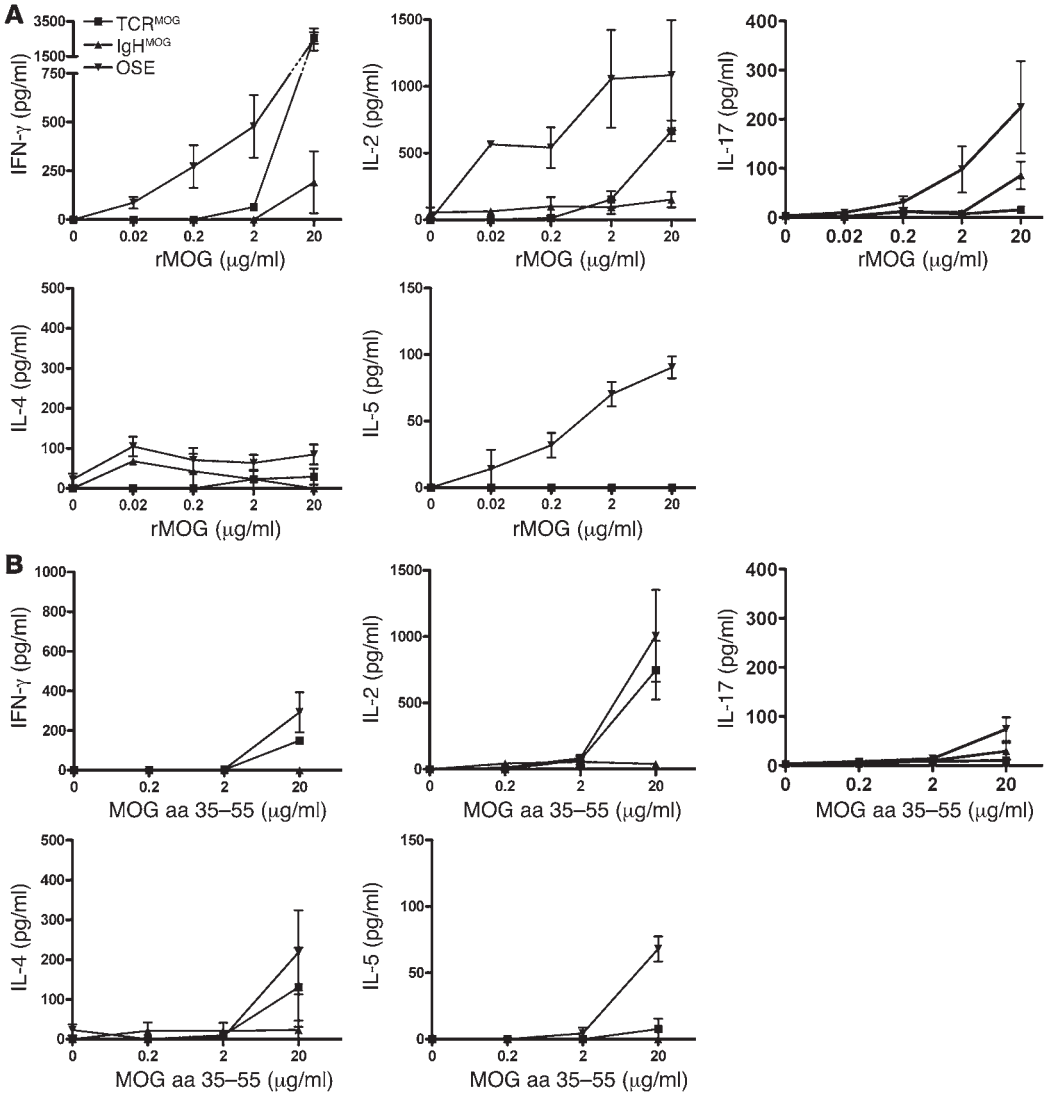

Figure 6

Cytokine production by transgenic splenocytes in vitro. (**A** and **B**) Splenocytes from OSE, TCR^{MOG}, and IgH^{MOG} mice were stimulated with increasing amounts of (**A**) rMOG or (**B**) MOG aa 35–55 peptide, and secreted IFN-γ, IL-2, IL-4, IL-5, and IL-17 cytokines were detected by ELISA. Representative results of a total of 7 OSE, 3 TCR^{MOG}, and 3 IgH^{MOG} animals analyzed during 3 independent experiments are shown. Error bars indicate SEM.

cell transgenic strains did. The question arises as to which events trigger EAE in OSE mice. In principle, both positive and negative triggers could be envisaged that weaken downregulatory control mechanisms. In human autoimmune disease the triggering events are commonly related to the inflammatory responses surrounding infection. The signals may include molecular mimicry among microbial and autoimmune determinants (13), microbial superantigens (14), and inflammatory milieus created by innate immune responses (15). The data from experimental models of spontaneous autoimmunity are, however, contradictory. Thus in transgenic mice with T cell receptors for MBP, spontaneous EAE was frequently noted in colonies with low hygienic standards, while mice of the same strain remained healthy when kept clean (11). In striking contrast, spontaneous type 1 diabetes mellitus in NOD mice arose more frequently in "clean" than in "dirty" colonies (4, 16). OSE mice from our colony, raised under either SPF or conventional conditions, developed spontaneous EAE at very similar rates.

EAE bouts have been elicited by signals of innate immune responses that mostly act on local APCs. For example, treatment of proteolipid protein–reactive, TCR transgenic mice with bacterial CpG or *Bordetella pertussis* toxin strikingly enhanced the incidence of spontaneous EAE (17). These stimuli did not affect EAE development in OSE mice (data not shown).

Alternatively, autoimmune disease has been precipitated in animals after weakening their regulatory T cell populations (18). Depletion of putative regulatory T cells from partly resistant B10.S mice increased the inducibility of EAE (19) or exacerbated established EAE in SJL/J mice (20). Applying current depletion protocols using anti–IL-2R and anti-GITR antibodies, we were unable to influence the occurrence of spontaneous Devic disease in our mouse colony. However, we noted a low frequency (<2%) of $CD4^+CD25^+CD69^-$ T cells in the mice (Supplemental Figure 8). Furthermore, we were unable to detect differences in the frequency of Foxp3 regulatory cell in healthy versus sick OSE mice (see Supplemental Figure 8 for details).

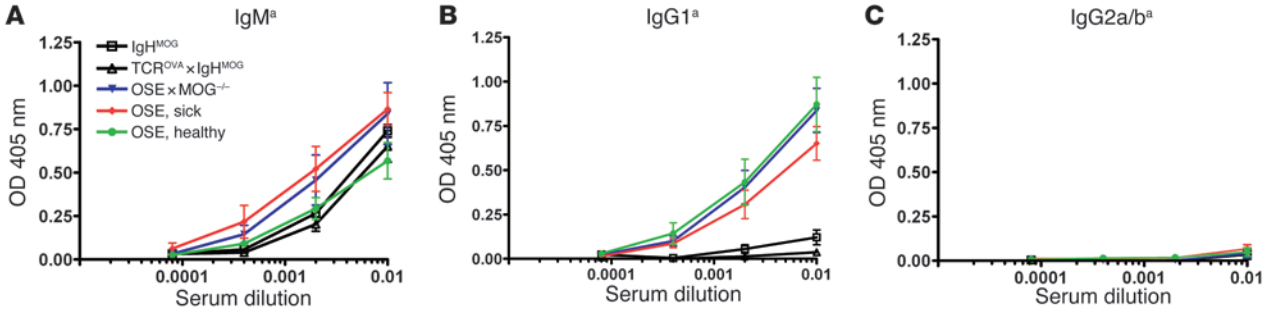

Figure 7
Relative concentrations of MOG-specific serum Ig antibodies in transgenic mice. MOG-binding antibodies were detected by ELISA in serially diluted sera obtained from healthy (n = 6) and sick (n = 7) OSE, healthy IgH^{MOG} (n = 6), healthy TCR^{OVA}×IgH^{MOG} (n = 6), and healthy OSE×MOG$^{–/–}$ (n = 3) mice. Sera (diluted at $10^{–2}$, $5 \times 10^{–2}$, $2.5 \times 10^{–3}$, and $1.25 \times 10^{–4}$) were incubated with plates precoated with rMOG. Bound anti-MOG Ig was detected by allotype-specific antibodies recognizing IgM^a (**A**), IgG1^a (**B**), or IgG2a/b^a (**C**). Mean absorbance at OD 405 nm is shown; error bars indicate SEM.

Human organ-specific autoimmune diseases like rheumatoid arthritis (21) and myasthenia gravis (22) seem to be the result of pathogenic interactions between autoreactive T and B lymphocytes. There is emerging evidence that, at least in a subset of MS cases, B and T cells cooperate to produce disease (2). Indeed, B cells and plasma cells are quite common components of MS lesions (23, 24). Further, the cerebrospinal fluid characteristically contains B cell products, the oligoclonal Ig bands, which seem to be the results of an antigen-driven immune response (25, 26). Finally, immunotherapies targeted to B cells and their products have been successful in classical MS (27) and Devic disease (28).

While to date EAE models have been used mainly to study the role of T cells in CNS autoimmunity, there are still only a few studies on autoimmune B cells. Several studies explored the contribution of B cells to the pathogenesis of EAE, either by depletion (29, 30) or by using transgenic mice with crippled Ig genes (31–33), but the role of autoantigen-specific B cells has been largely neglected.

The double-transgenic mouse strain described here, which we believe to be novel, fills this gap. OSE mice are double-transgenic for T and B cell receptors specific for the same myelin autoantigen, MOG. Autoimmune T and B cells thus may interact on several levels to create disease. First, antigen-specific B cells are known to efficiently capture even highly diluted protein antigen via their surface Ig receptors, to process the antigen, and then to present it to specific T cells in the context of appropriate MHC determinants (34). This is definitely the case in OSE mice. The transgenic B cells have receptors that bind only conformational epitopes formed by rMOG protein (8) and fail to bind MOG aa 35–55 peptide. Consequently, in these mice, the MOG-specific B cells were able to pick up and concentrate rMOG present at enormous dilutions and present it efficiently to specific T cells. However, the same B cells failed to concentrate MOG peptide.

The role of MOG-specific B cells is, however, not restricted to antigen presentation. We have shown that in double-transgenic spleen cultures, both T and B cells responded to MOG by activation and proliferation. Furthermore, MOG-specific T cells, activated by MOG, can drive their B cell partners into differentiation pathways, toward either Ig-producing plasma cells or long-lived memory B cells. Further, these T cell/B cell interactions control Ig affinity maturation and isotype switching, as indicated by our finding that anti-MOG Igs underwent a class switch from IgM to IgG1 — a switch pattern commonly related to Th2 responses — in OSE mice. This did not occur in IgH^{MOG} mice or in double-transgenic TCR^{OVA}×IgH^{MOG} mice. Remarkably, however, OSE mice showed a cytokine pattern (high levels of IFN-γ and IL-2, low levels of IL-5 and IL-17, and no detectable IL-4) that dominated the transgenic T cells both in vitro and in the CNS milieu. Factors other than the known switch cytokines must have contributed to the IgG1 isotype switch of anti-MOG autoantibodies.

Following conventional concepts, the Ig switch to IgG1 should be the consequence of presentation and recognition of the nominal autoantigen, MOG, between both partner cells. It is thus another major surprise that the IgG1 switch of anti-MOG autoantibodies was seen in OSE mice not only on a MOG$^{+/+}$ background but also on a MOG$^{–/–}$ background. This raises the question of the (auto)antigen linking T and B cells in vivo. In a previous study of double-transgenic mice expressing the IgH^{MOG} gene replacement plus the light chain from the donor hybridoma, Litzenburger et al. observed B cell receptor editing (35), a phenomenon involving B cell contact with self antigen (36). MOG-reactive B cells showed evidence of receptor editing in both MOG$^{+/+}$ and MOG$^{–/–}$ mice, a finding that suggests a non-MOG self protein mimicking MOG epitopes (35).

In OSE mice, the particular localization of lesions in the optic nerve and in the spinal cord differs from most actively induced or passively transferred EAE variants. Presumably, lesion distribution depends both on the nature of the target autoantigen and on genetic factors. While classic EAE induced in Lewis rats by MBP-specific T cells affects the spinal cord in a caudocranial gradient of intensity, other CNS autoantigens produce very different patterns in the same strain (37). Conversely, immunization of BN rats with rMOG produces EAE with distribution like that in OSE mice, while sensitization of DA rats results in inflammation throughout the CNS (38). Furthermore, single-transgenic TCR^{MOG} mice frequently show isolated optic neuritis, but rarely spinal cord lesions (5).

The distribution of the demyelinating lesions within the optic nerve and the spinal cord along with their particular cellular composition in our transgenic mice are similar to that in Devic disease. However, TCR^{MOG}×IgH^{MOG} double-transgenic OSE mice were not able to replicate all aspects of the complex clinical and pathological patterns observed in human Devic disease. Most importantly, in Devic disease long monofocal lesions are observed that are predominantly located in the cervical spinal cord segments. Highly destructive and necrotic lesions are symmetrical and mainly affect the central portions of the spinal cord over several segments. Despite

impressive and severe pathology in OSE mice, we were unable to see such devastating pathology (Figure 2), probably due in part to the fact that affected animals rapidly developed severe clinical symptoms after onset of disease, often requiring the early scarification of such animals (see Supplemental Figure 2). Furthermore, human Devic disease seems to be associated with massive perivascular IgM, IgG, and complement deposition, which are not specifically located on myelin sheaths. We, however, were unable to detect comparable complement deposition within the CNS of sick OSE mice (data not shown). Antibodies binding to aquaporin-4, which have been recently described in the sera of Devic disease patients (39), seemed to be absent in OSE mice (data not shown). This discrepancy may, however, be of limited importance, as anti-aquaporin antibodies were missing in about 30% of Devic patient sera. Moreover, the distribution of aquaporin within the human CNS does not coincide with the distribution of demyelinating lesions in Devic disease (39, 40).

OSE mice offer important new features, which will make them of use for a number of purposes. Most interestingly, they may lend themselves to the study of mechanisms that precipitate spontaneous autoimmune disease. OSE mice may also be useful for exploring factors that determine the localization of lesions and their cellular composition. Finally, as a model of spontaneous, non–adjuvant-induced autoimmunity, OSE mice may be helpful in the preclinical validation of novel therapies of autoimmune CNS disease.

Methods

Animals and disease scoring. The transgenic IgH^{MOG} (also referred to as Th; ref. 8), TCR^{MOG} (also referred to as 2D2; ref. 5), and $MOG^{-/-}$ mice (10) along with C57BL/6 mice were bred in the animal facilities of the Max Planck Institute of Biochemistry. TCR^{MOG} mice were generated directly on the C57BL/6 genetic background (5). IgH^{MOG} and $MOG^{-/-}$ mice were originally made using 129-derived ES cells but were backcrossed against the C57BL/6 strain for more than 12 and 8 generations, respectively. Homozygous TCR^{OVA} mice ($n = 6$) were purchased from Jackson Laboratory.

F1 animals resulting from the intercross of IgH^{MOG} with TCR^{MOG} or TCR^{OVA} mice were weighed and examined every 2–3 days for clinical signs of disease. Clinical scoring of animals was according to the classic EAE disease determination: 0, healthy animal; 1, animal with a flaccid tail; 2, animal with impaired righting reflex and/or gait; 3, animal with 1 paralyzed hind leg; 4, animal with both hind legs paralyzed; 5, moribund animal or death of the animal after preceding clinical disease.

All animal procedures used in this report were in accordance with guidelines of the committee on animals of the Max Planck Institute for Neurobiology and with the license of the Regierung von Oberbayern (Munich, Germany).

Antigens. rMOG was purified from bacterial inclusion bodies (41). MOG aa 35–55 peptide was synthesized at BioTrend, Germany.

Immunization of animals. Mice were injected s.c. at the tail base with an emulsion of equal amounts of CFA and 200 μg MOG aa 35–55 in PBS. CFA was supplemented with 5 mg/ml *Mycobacterium tuberculosis* (strain H37Ra). Pertussis toxin (400 ng) was injected i.p. on days 0 and 2 relative to immunization.

Histological analysis. Animals were perfused with 4% paraformaldehyde in PBS, stored in the same fixative for 24 hours, and then washed twice with PBS. Brain and spinal cord tissue was dissected and in part embedded in paraffin or snap frozen for immunocytochemistry. Adjacent serial sections were stained with H&E, luxol fast blue, or Bielschowsky silver impregnation.

Immunohistochemistry. Immunohistochemical stainings were performed as described previously (42). Tissue sections (8–12 μm) were incubated with primary rat antibodies recognizing mouse CD4, CD11b, CD8a, IgM, CD19, or B220 (all obtained from BD Biosciences — Pharmingen). A secondary biotinylated anti-rat antibody, a streptavidin-HRP complex (both from Vector Laboratories), and diaminobenzidine (Zymed) allowed the cell type specific detection of mononuclear cells. Slides were counterstained with Meyer's hematoxylin and embedded in AquaMount (Fisher Scientific) prior to microscopic analysis.

Flow cytometric analysis. Mononuclear cells were isolated from the CNS by Percoll gradient centrifugation. For the detection of cell surface markers by FACS analysis, cells were stained with fluorochrome-labeled antibodies (BD Biosciences — Pharmingen; see Supplemental Methods for details). MOG-binding cells were detected with biotinylated rMOG protein (41) and a streptavidin-allophycocyanin complex (BD Biosciences — Pharmingen). Intracellular Foxp3 staining was performed according to the manufacturer's instructions (eBioscience). Data acquisition was done with a FACSCalibur system and CellQuest software (BD). For data analysis CellQuest software and WinMDI software (version 2.8; http://facs.scripps.edu/software.html) were used.

In vitro proliferation assay. Single-cell suspensions from spleens were prepared, and 2×10^5 cells/well were seeded in 96-well, round-bottomed plates in a total volume of 200 μl complete RPMI medium containing 10% FCS (Invitrogen). After a culture period of 48 hours, 1 μCi ^{3}H-labeled thymidine was added per well. Samples were harvested 16 hours later, and tritium incorporation was measured. Each sample was run in triplicate.

Cell purification. Lymphocyte subpopulations were purified from the spleens of transgenic mice using B cell or T cell Negative Selection kits (Dynal). Their viability and purity were evaluated by FACS analysis. The cell purification procedure generally resulted in cell populations that were more than 90% pure.

CFSE labeling of lymphocytes. Cells (2×10^7) were incubated at 37°C for 10 minutes with 1% FCS/PBS containing 5 μM CFSE (Invitrogen) and were subsequently washed extensively with cold PBS.

ELISA. Cells were plated and stimulated as described for proliferation assays. After 72 hours cell supernatants were collected. Cytokine concentrations were determined using matching antibody pairs for mouse IL-2, IFN-γ, IL-4, IL-5 (BD Biosciences — Pharmingen), and IL-17 (R&D Systems). For colorimetric cytokine determination, 2,2′-azino-bis (3-ethylbenzthiazoline-6-sulphonic acid (ABTS; Sigma-Aldrich) was used as a substrate, and plates were read at 405 nm.

Determination of serum titers of MOG-specific antibodies. Serially diluted serum collected from transgenic mice were transferred to 96-well ELISA plates (Nunc) precoated with rMOG. After extensive washes, bound Ig was detected by a sandwich consisting of a biotinylated allotype- and isotype-specific anti-mouse Ig (all BD Biosciences — Pharmingen; see Supplemental Methods for details) and a streptavidin-HRP complex (BD Biosciences — Pharmingen). ABTS was used as a color substrate that was measured at 405 nm.

Quantitative real-time TaqMan PCR analysis. Total RNA was isolated from the spinal cord and optic nerves by TRI Reagent extraction (Sigma-Aldrich) and, following DNase I treatment, was converted into cDNA using either hexanucleotide or oligo-dT primers and SuperScript II Reverse Transcriptase (Invitrogen). Sense and antisense primers in combination with FAM/TAMRA TaqMan probes and gene-specific primers (synthesized at Metabion) were used for PCR analysis. A list of used primer sequences for the IFN-γ, TNF-α, IL-4, IL-5, IL-10, IL-13, IP-10, eotaxin, Foxp3, and GAPDH genes is provided in Supplemental Methods. Where possible the primer/probe sequence combinations spanned contact sequences of subsequent exons. For amplification the ABsolute QPCR mix was used (ABgene). Each reaction was run in triplicate on an ABI 5700 machine (Applied Biosystems) and was normalized to housekeeping gene GAPDH transcripts. Primary data was analyzed with GeneAmp SDS 5700 software (Applied Biosystems).

Statistics. Descriptive statistical analysis was performed using Excel 2003 (Microsoft) and Prism version 4 (GraphPad) software. Differential

EAE incidence was analyzed by log-rank test (by an in-built survival curve analysis from Prism version 4). *P* values less than 0.05 were considered to be significant.

Acknowledgments

We thank Irene Arnold-Ammer for exceptional technical assistance; Edgar Meinl, Florian Kurschus, and Klaus Dornmair for critical review of the manuscript; Estelle Bettelli and Vijay Kuchroo for providing 2D2 transgenic mice; Danielle Pham-Dinh for $MOG^{-/-}$ animals; and Shimon Sakaguchi for the DTA-1 and PC61 hybridoma. This work was supported in part by the Max Planck society, the Deutsche Forschungsgemeinschaft (SFB 571), and the National Multiple Sclerosis Society (grant RG3335A1/T).

Received for publication February 23, 2006, and accepted in revised form June 13, 2006.

Address correspondence to: Andreas Holz or Hartmut Wekerle, Department of Neuroimmunology, Max Planck Institute for Neurobiology, Am Klopferspitz 18, D-82152 Martinsried, Germany. Phone: 48-89-8578-3561; Fax: 49-89-8995-0170; E-mail: holz@neuro.mpg.de (A. Holz). Phone: 49-89-8578-3551; Fax: 49-89-8578-3790; E-mail: hwekerle@neuro.mpg.de (H. Wekerle).

Andreas Holz's present address is: Technical University of Braunschweig — Biocenter, Department of Cell and Molecular Biology, Braunschweig, Germany.

1. O'Riordan, J.I., et al. 1996. Clinical, CSF and MRI findings in Devic's neuromyelitis optica. *J. Neurol. Neurosurg. Psychiatry.* **60**:382–387.
2. Lassmann, H., Brück, W., and Lucchinetti, C. 2001. Heterogeneity of multiple sclerosis pathogenesis: implications for diagnosis and therapy. *Trends Mol. Med.* **7**:115–121.
3. Kurtzke, J.F. 1993. Epidemiologic evidence for multiple sclerosis as an infection. *Clin. Microbiol. Rev.* **6**:382–427.
4. Bach, J.-F. 2002. The effect of infections on susceptibility to autoimmune and allergic diseases. *N. Engl. J. Med.* **347**:911–920.
5. Bettelli, E., et al. 2003. Myelin oligodendrocyte glycoprotein-specific T cell receptor transgenic mice develop spontaneous autoimmune optic neuritis. *J. Exp. Med.* **197**:1073–1081.
6. Linington, C., Webb, M., and Woodhams, P.L. 1984. A novel myelin-associated glycoprotein defined by a mouse monoclonal antibody. *J. Neuroimmunol.* **6**:387–396.
7. Linington, C., Bradl, M., Lassmann, H., Brunner, C., and Vass, K. 1988. Augmentation of demyelination in rat acute allergic encephalomyelitis by circulating mouse monoclonal antibodies directed against a myelin/oligodendrocyte glycoprotein. *Am. J. Pathol.* **130**:443–454.
8. Litzenburger, T., et al. 1998. B lymphocytes producing demyelinating autoantibodies: development and function in gene-targeted transgenic mice. *J. Exp. Med.* **188**:169–180.
9. Barnden, M.J., Allison, J., Heath, W.R., and Carbone, F.R. 1998. Defective TCR expression in transgenic mice constructed using cDNA-based α- and β-chain genes under the control of heterologous regulatory elements. *Immunol. Cell Biol.* **76**:34–40.
10. Delarasse, C., et al. 2003. Myelin/oligodendrocyte glycoprotein–deficient (MOG-deficient) mice reveal lack of immune tolerance to MOG in wild-type mice. *J. Clin. Invest.* **112**:544–553. doi:10.1172/JCI200315861.
11. Goverman, J., et al. 1993. Transgenic mice that express a myelin basic protein-specific T cell receptor develop spontaneous autoimmunity. *Cell.* **72**:551–560.
12. Lafaille, J., Nagashima, K., Katsuki, M., and Tonegawa, S. 1994. High incidence of spontaneous autoimmune encephalomyelitis in immunodeficient anti-myelin basic protein T cell receptor mice. *Cell.* **78**:399–408.
13. Oldstone, M.B.A. 1987. Molecular mimicry and autoimmune disease. *Cell.* **50**:819–820.
14. Schiffenbauer, J., Soos, J.M., and Johnson, H. 1998. The possible role of bacterial superantigen in the pathogenesis of autoimmune disorders. *Immunol. Today.* **19**:117–120.
15. Bachmann, M.F., and Kopf, M. 2001. On the role of the innate immunity in autoimmune disease. *J. Exp. Med.* **193**:F47–F50.
16. Pozzilli, P., Signore, A., Williams, A.J.K., and Beales, P.E. 1993. NOD mouse colonies around the world - recent facts and figures. *Immunol. Today.* **14**:193–196.
17. Waldner, H., Collins, M., and Kuchroo, V.K. 2004. Activation of antigen-presenting cells by microbial products breaks self tolerance and induces autoimmune disease. *J. Clin. Invest.* **113**:990–997. doi:10.1172/JCI200419388.
18. Bach, J.-F. 2003. Regulatory T cells under scrutiny. *Nat. Rev. Immunol.* **3**:189–198.
19. Reddy, J., et al. 2004. Myelin proteolipid protein-specific CD4+CD25+ regulatory cells mediate genetic resistance to experimental autoimmune encephalomyelitis. *Proc. Natl. Acad. Sci. U. S. A.* **101**:15434–15439.
20. Kohm, A.P., Williams, J.S., and Miller, S.D. 2004. Ligation of the glucocorticoid-induced TNF receptor enhances autoreactive $CD4^+$ T cell activation and experimental autoimmune encephalomyelitis. *J. Immunol.* **172**:4684–4690.
21. Dörner, T., and Burmester, G.R. 2003. The role of B cells in rheumatoid arthritis: mechanisms and therapeutic targets. *Curr. Opin. Rheumatol.* **15**:246–252.
22. Hohlfeld, R., and Wekerle, H. 1999. The immunopathogenesis of myasthenia gravis. In *Myasthenia gravis and myasthenic syndromes*. A.G. Engel, editor. Oxford University Press. Oxford, United Kingdom. 87–110.
23. Esiri, M.M. 1980. Multiple sclerosis: a quantitative and qualitative study of immunoglobulin-containing cells in the central nervous system. *Neuropathol. Appl. Neurobiol.* **6**:9–21.
24. Baranzini, S.E., et al. 1999. B cell repertoire diversity and clonal expansion in multiple sclerosis brain lesions. *J. Immunol.* **163**:5133–5144.
25. Qin, Y.F., et al. 2003. Intrathecal B-cell clonal expansion, an early sign of humoral immunity, in the cerebrospinal fluid of patients with clinically isolated syndrome suggestive of multiple sclerosis. *Lab. Invest.* **83**:1081–1088.
26. Owens, G.C., et al. 2003. Single-cell repertoire analysis demonstrates that clonal expansion is a prominent feature of the B cell response in multiple sclerosis cerebrospinal fluid. *J. Immunol.* **171**:2725–2733.
27. Keegan, M., et al. 2005. Relation between humoral pathological changes in multiple sclerosis and response to therapeutic plasma exchange. *Lancet.* **366**:579–582.
28. Cree, B.A.C., et al. 2005. An open label study of the effects of rituximab in neuromyelitis optica. *Neurology.* **64**:1270–1272.
29. Gausas, J., Paterson, P.Y., Day, E.D., and Dal Canto, M.C. 1982. Intact B-cell activity is essential for complete expression of experimental allergic encephalomyelitis in Lewis rats. *Cell. Immunol.* **72**:360–366.
30. Myers, K.J., Sprent, J., Dougherty, J.P., and Ron, Y. 1992. Synergy between encephalitogenic T cells and myelin basic protein-specific antibodies in the induction of experimental autoimmune encephalomyelitis. *J. Neuroimmunol.* **41**:1–8.
31. Wolf, S.D., Dittel, B.N., Hardardottir, F., and Janeway, C.A. 1996. Experimental autoimmune encephalomyelitis induction in genetically B cell-deficient mice. *J. Exp. Med.* **184**:2271–2278.
32. Hjelmström, P., Juedes, A.E., Fjell, J., and Ruddle, N.H. 1998. B cell deficient mice develop experimental allergic encephalomyelitis with demyelination after myelin oligodendrocyte glycoprotein immunization. *J. Immunol.* **161**:4480–4483.
33. Lyons, J.-A., San, M., Happ, M.P., and Cross, A.H. 1999. B cells are critical to induction of experimental allergic encephalomyelitis by protein but not by a short encephalitogenic peptide. *Eur. J. Immunol.* **29**:3432–3439.
34. Lanzavecchia, A. 1990. Receptor-mediated antigen uptake and its effects on antigen presentation to class II-restricted T lymphocytes. *Annu. Rev. Immunol.* **8**:773–794.
35. Litzenburger, T., et al. 2000. Development of MOG autoreactive transgenic B lymphocytes: receptor editing in vivo following encounter of a self-antigen distinct from MOG. *J. Immunol.* **165**:5360–5366.
36. Verkoczy, L.K., Mårtensson, A.S., and Nemazee, D. 2004. The scope of receptor editing and its association with autoimmunity. *Curr. Opin. Immunol.* **16**:808–816.
37. Berger, T., et al. 1997. Experimental autoimmune encephalomyelitis: the antigen specificity of T-lymphocytes determines the topography of lesions in the central and peripheral nervous system. *Lab. Invest.* **76**:355–364.
38. Storch, M.K., et al. 1998. Autoimmunity to myelin oligodendrocyte glycoprotein in rats mimics the spectrum of multiple sclerosis pathology. *Brain Pathol.* **8**:681–694.
39. Lennon, V.A., Kryzer, T.J., Pittock, S.J., Verkman, A.S., and Hinson, S.R. 2005. IgG marker of optic-spinal multiple sclerosis binds to the aquaporin-4 water channel. *J. Exp. Med.* **202**:473–477.
40. Lennon, V.A., et al. 2004. A serum autoantibody marker of neuromyelitis optica: distinction from multiple sclerosis. *Lancet.* **364**:2106–2112.
41. Adelmann, M., et al. 1995. The N-terminal domain of the myelin oligodendrocyte glycoprotein (MOG) induces acute demyelinating experimental autoimmune encephalomyelitis in the Lewis rat. *J. Neuroimmunol.* **63**:17–27.
42. Holz, A., Brett, K., and Oldstone, M.B.A. 2001. Constitutive β-cell expression of IL-12 does not perturb self-tolerance but intensifies established autoimmune diabetes. *J. Clin. Invest.* **108**:1749–1758. doi:10.1172/JCI200113915.